Piotr Sakiewicz[1], Krzysztof Piotrowski[2*], Sylwester Kalisz[3]

Neural network prediction of parameters of ashes reused within the Circular Economy frame

[1] Institute of Engineering Materials and Biomaterials, Division of Nanocrystalline and Functional Materials and Sustainable Pro-ecological Technologies, Faculty of Mechanical Engineering, Silesian University of Technology, Konarskiego 18A, 44-100 Gliwice, Poland, e-mail: piotr.sakiewicz@polsl.pl
[2] Department of Chemical Engineering and Process Design, Faculty of Chemistry, Silesian University of Technology, ks. M. Strzody 7, 44-100 Gliwice, Poland, e-mail: krzysztof.piotrowski@polsl.pl
[3] Institute of Power Generation and Turbomachinery, Faculty of Energy and Environmental Engineering, Silesian University of Technology, Konarskiego 18, 44-100 Gliwice, Poland, e-mail: sylwester.kalisz@polsl.pl

* Corresponding author: krzysztof.piotrowski@polsl.pl

Abstract:

Artificial neural networks were used for prediction of three biomass ash fusion temperatures: initial deformation temperature IDT, hemispherical temperature HT and softening temperature FT based on chemical composition of the ash. Applicability of 400 neural network configurations (of linear, MLP, RBF and GRNN types) was verified statistically. Multilayer perceptron with 12 inputs representing fractions of ash compounds, 11 hidden neurons and three outputs (IDT, HT, FT) proved to be the optimal model configuration. Statistical analysis suggested also, that considering intrinsic dispersion within raw experimental data (literature data supplemented with the authors' own results describing halloysite addition effect), quality of the resulting 3-output IDT-HT-FT model (IDT prediction with R^2 0,615, HT with R^2 0,756 and FT with R^2 0,729) could be regarded satisfactory for the identification and generalization of the discussed relationships. Analysis of the neural model sensitivity in respect to input variables demonstrated, that the most important factors affecting all ash transition temperatures in 3-output IDT-HT-FT model were K_2O, SiO_2, CaO and Al_2O_3 fractions. Moreover, individual sensitivity in respect to IDT, HT and FT temperatures slightly varied (characteristics provided by independently established 1-output networks – IDT model, HT model and FT model, respectively). Statistically verified neural network working as 3-output IDT-HT-FT model can be applied in various computational tasks in biofuels energy sector required by Industry 4.0 principles, as well as in selected Circular Economy problems.

Key words: artificial neural networks, Circular Economy, ash fusion temperature, Industry 4.0, predictive model.

Introduction

Biofuels represent important sector in the present world's energetic market [1]. These can be co-fired with coal [2] or converted into more convenient forms in processes of anaerobic digestion or by means of thermal decomposition technologies like pyrolysis or gasification. Neutral towards greenhouse effect, these are regarded to be environmentally friendly, providing sustainable development of modern industry. Especially important is also reusing or recycling of solid residues (ashes) after biomass fuel burning according to Circular Economy rules and principles.

Chemical composition of the ashes, the residuals derived from biomass burning (especially their phase composition) is an important ash quality parameter. Ash represents mixture of inorganic and organic compounds, of various combinations and proportions [3]. It covers amorphous, semi-crystalline and crystalline species, as well as char. Presence of complex organic liquids inclusions within the solid inorganic/organic structure makes that the system is heterogeneous. Its complexity can be confirmed by the fact, that 229 identified phases or minerals were found analytically in biomass ash structure, depending on initial composition of biomass, its origin and burning process parameters, as well as reaction/transformations schemes depending on thermodynamic conditions applied [4-7]. The most common compounds of the typical ashes are: silicates, oxides, hydroxides, oxyhydroxides,

sulphates, sulphides, sulphosalts, sulphites, thiosulphates, phosphates, carbonates, bicarbonates, nitrates, chlorides, chlorites, chlorates, glass, some minor inorganic/organic phases/minerals [4]. Additional factors necessary for considering are particle morphology, shape and size distributions, which are also complex functions of both intrinsic biomass properties and sequence of technological processes and their parameters (mainly residence time, pressure and temperature, reaction schemes [8]), as well as presence of appropriately selected and dosed additives [9-11].

Ash composition and the ash-derived properties are the key-aspects in postprocessed utilization strategy of the biomass-derived ashes. It may include reusing/recycling [12-15] (according to Circular Economy standards and principles), as well as safe disposal (neutral to natural environment, assuring prevention of its contamination) [4,16]. Depending on ash composition, various disadvantageous phenomena are observed, like sintering, agglomeration, melting, clinkering, fouling, corrosion and slagging, as well as erosion and abrasion [17].

Different biomass ashes, depending on their composition, show different characteristic ash temperatures – thus consequently different physicochemical characteristics [18]. Prediction of thermodynamic behavior of the ash is a complex task – various approaches were reported in literature using empirical indices, coefficients and their unique combinations [19,20].

The term ash fusion temperature (AFT) is in practice characterized by various specific temperature points. These are usually: deformation temperature (DT), hemispherical temperature (HT), softening temperature (ST), as well as flow temperature (FT). Both various chemical composition of the fuel and sequence of processes with their parameters affect these temperatures values. Since these thermal parameters are important for practical applications (like recommended operation ranges, optimal process thermal efficiency, etc.), some models are required for possibly precise and reliable prediction of these parameters. Complex interactions between chemical composition of the raw biofuel, its natural structure, proportions of inorganic and organic fractions, as well as selected thermal processing technology affect, besides chemical and phase transformations of the constituents, also changes in solid matrix, diffusional and kinetic effects in heterogeneous matrix, as well as secondary reactions – all these define extremely complex interactions and intrinsic feedbacks resulting in diversified characteristic temperature parameters of the ash. Also commonly observed inhomogeneous composition of the available biofuels, co-substrates, additives and/or modifying agents, representing together “raw materials” in energy production processes define additional complexity of this technical problem. These examples suggest necessity of optimization of the technological processes of burning and their close integration with modern computer systems supervising the energy production processes in real time. One of such data processing systems and modeling tools, making such integration and control possible, are artificial neural networks (ANNs) being main element of the hybrid, ANN-based algorithms, making use of unique artificial intelligence advantages. These provide real possibility of rational selection of parameters involved in prediction, steering and control of the energetic burning processes, making them comply with global strategy of Industry 4.0.

Considering the intrinsic complexity of the data, artificial neural networks were thus proposed for the examination and exploring of the hidden data structure, then for modeling of these relations, especially for identification of the interrelations and feedbacks within the input-output data.

Neural networks are applied, among others, for modeling of various systems, objects or processes where one is not able to dispose any information about nature and strength of internal connections scheme within the system. This way classical regression techniques, based on imposing of a rigid model frame followed by calculation of these model coefficients, are not applicable. Instead, using neural network computations only representative set of data resulting e.g. from sampling of the object in different conditions is demanded. Using neural network approach it is even not necessary to assume any preliminary model frame since during net training various structures are tested and the network itself identifies and generalizes the knowledge concerning hidden interrelations and intrinsic feedbacks in the available representative (e.g. measurements, experimental) dataset. Theoretical background of neural networks structure, performance and training algorithms, with their mathematical details are presented e.g. in other authors’ works [21-28].

In literature one can find some examples of neural networks application in this field. For example neural nets were used for prediction of properties (or their changes) of building materials (concrete, cement, reinforced concrete) after ash addition [29-34], prediction of calorific and ash

values of fuel [35] and process conditions (e.g. ash agglomerating fluidized bed gasifier [36]), estimation of ash content for the given fuel [37], forecasting of tribological behaviour of rice husk ash reinforced aluminum alloy matrix composites [38], as well as estimation of strength of geopolymers [39].

In accessible scientific literature one can find also some tests of neural network models applicability for forecasting of ash transition temperatures. However, all are focused rather on the coal ash properties based on fuel from various sources, what is then unequivocally reflected by chemical composition of the ashes. In [40] authors examined fusion temperature of coal ash based on industrial data. Neural network technique provided better results than various empirical approaches. As the neural network model inputs the following parameters were used: SiO_2, Al_2O_3, Fe_2O_3, CaO, MgO (optionally with additional TiO_2, K_2O, Na_2O, P_2O_5, SO_3) mineral fractions. Output was represented by ash softening temperature (ST). Other work [41] focused on coal ash fusion temperature using net trained with backpropagation error (BP) algorithm coupled with the ant colony optimization algorithm. As the inputs seven oxide fractions were used, covering SiO_2, Al_2O_3, Fe_2O_3, CaO, MgO, (K_2O+Na_2O) and TiO_2, whereas fusion temperature was used as the output of the neural network model. The 10 hidden neurons were regarded to provide satisfactory prediction results and data structure mapping. Another work [42], also analyzing coal ash fusion temperature, reported application of three-layer BP network, with seven inputs representing fractions of SiO_2, Al_2O_3, Fe_2O_3, CaO, MgO, TiO_2, (K_2O+Na_2O) in chemical composition of coal ash, with one output neuron providing the information about softening temperature value. Eight hidden neurons were considered to be satisfactory enough for precise projection and modeling of this specific dataset.

Calculations

The data being the basis for neural network model construction were represented by coupled set published in [19] and the authors' own data [43] covering burning experiments with addition of halloysite (more information about properties of halloysite and its potential applications can be found in other authors works' [44-46]). These represented information from chemical analysis of postprocessed ashes after burning of various types of natural biomass, with corresponding characteristic temperatures. This data set [19] was supplemented with some information concerning own experiments, assuming the same form of data vectors (12 inputs coupled with 3 output temperatures – see Table 1). The original 101 data vectors of structure presented in Table 1 were normalized to 100%. Statistical characteristics of the database are presented in Table 1.

Table 1
Statistical characteristics of the dataset used for neural network models preparation.

	Ash composition after biomass burning (dry weight basis)												Ash melting temperatures [°C]		
	SiO_2	CaO	K_2O	P_2O_5	Al_2O_3	MgO	Fe_2O_3	SO_3	N_2O	TiO_2	S_d	Cl	IDT	HT	FT
	Input data												Output data		
Mean	29,584	21,519	21,050	5,700	4,285	6,127	3,208	5,390	1,957	0,804	0,167	0,209	1151,3	1296,7	1323,5
Median	28,383	15,363	18,271	3,878	2,582	4,556	1,809	3,530	0,998	0,240	0,080	0,080	1173	1249	1269
St deviation	23,639	15,792	15,507	6,091	4,382	5,007	4,764	6,280	4,017	2,359	0,310	0,365	177,8	132,2	117,6
Minimum	0	0,968	0,227	0	0,010	0,190	0	0,360	0	0	0,010	0	750	1070	1070
Maximum	94,291	72,296	63,874	39,918	14,837	38,182	36,314	45,771	29,755	21,914	2,276	3,017	1500	1500	1500

Analyzing the model output parameters – IDT, HT and FT, especially comparing mean (or median) value with standard deviation for each parameter individually, one can notice relatively large dispersion of the output data, what can potentially affect the model performance. On the other hand, the minimum and maximum values of input parameters suggest, that the neural model can be potentially used in a wide range of input parameters values.

Taking under consideration potentially complex intrinsic structure of the data, as well as presented and emphasized in literature difficulties and problems in correct modeling of the data using classical approaches based on statistics and regression rules (the reporting R^2 varied within the 0,058 – 0,708 range [19] depending on various combinations of indices), some alternative approach was suggested – artificial neural networks – computational method based on artificial intelligence approach.

Results and discussion

Calculations covering formulation of diversified neural networks structures and types, followed by their training, validating and testing were done in *Statistica Neural Networks* software environment. Main idea of the neural model was to predict three characteristic ash melting temperatures (defined as IDT, HT, FT) based only on chemical characteristics of the biomass represented by fractions (in %, dry weight basis [19]) of: SiO_2, CaO, K_2O, P_2O_5, Al_2O_3, MgO, Fe_2O_3, SO_3, N_2O, TiO_2, S_d and Cl (assuming that Σ=100%). These temperatures represented: IDT – initial deformation temperature, HT – hemosphere temperature and FT – fluid (softening) temperature. The available 101 numerical input-output data vectors representative to the system, were randomly divided into training, validating and testing subsets, assuming proportions of 50% : 25% : 25%.

Various neural networks topologies were systematically tested and compared. These were: linear networks, multilayer perceptrons (MLPs), radial basis functions (RBFs) and general regression neural networks (GRNNs). Neural network structures were trained in supervised mode, based on appropriate to each configuration training algorithms, including: pseudoinversion (PI), backpropagation error (BP), conjugate gradient (CG), *k*-means (KM), *k*-neighbors (KN) and subsample (SS) ones. Some exemplary results are presented in Table 2. Both networks with full 12 inputs (see Table 1) and net structures with reduced inputs number (considering to the procedure of input vector dimension cutting according to performed on-line, strictly connected with training algorithm analysis of inputs importance hierarchy) were considered during systematic verification procedure.

Table 2
Exemplary artificial neural network configurations tested.

No	Network type and configuration (topology)	Quality – training subset	Quality – validating subset	Quality – testing subset	Error – training subset	Error – validating subset	Error – testing subset	Details of neural network's training sequence
1	Linear 4-3	0,8733	0,9682	0,8864	0,2546	0,2868	0,2556	PI
2	Linear 6-3	0,8242	0,9436	0,8394	0,2476	0,2881	0,2460	PI
3	Linear 8-3	0,7887	0,9548	0,8305	0,2376	0,2937	0,2432	PI
4	Linear 10-3	0,6985	0,9587	0,8718	0,2152	0,3018	0,2489	PI
5	Linear 11-3	0,6981	0,9866	0,8779	0,2148	0,3133	0,2530	PI
6	Linear 12-3	0,6998	0,9876	0,8778	0,2210	0,3105	0,2566	PI
7	MLP 8-3-3	0,4866	0,9124	0,8316	0,1087	0,2064	0,1854	BP100, CG77
8	MLP 12-11-3	0,4482	0,7869	0,6883	0,1167	0,2064	0,1658	BP100, CG34
9	MLP 12-12-3	0,4026	0,9171	0,7821	0,0864	0,2055	0,1783	BP100, CG55
10	MLP 4-9-4-3	0,6477	0,8362	0,6813	0,1651	0,2032	0,1691	BP100, CG84
11	MLP 11-11-11-3	0,4068	0,8786	0,6273	0,0948	0,1902	0,1789	BP100, CG37
12	MLP 12-13-11-3	0,3525	0,8557	0,6564	0,0841	0,2029	0,1659	BP100, CG39
13	MLP 12-13-13-3	0,3290	0,9388	0,6067	0,0936	0,2059	0,1868	BP100, CG30
14	RBF 11-4-3	0,8110	1,1831	0,8168	0,0058	0,0084	0,0057	KM, KN, PI
15	RBF 11-5-3	0,8040	1,1478	0,8309	0,0057	0,0083	0,0059	KM, KN, PI
16	RBF 11-7-3	0,7469	1,1159	0,8047	0,0054	0,0087	0,0056	KM, KN, PI
17	RBF 11-9-3	0,5904	0,9680	0,7325	0,0042	0,0066	0,0049	KM, KN, PI
18	RBF 11-14-3	0,5511	1,0547	0,7250	0,0041	0,0067	0,0047	KM, KN, PI
19	GRNN 2-51-4-3	0,8791	0,9588	0,8889	0,0059	0,0068	0,0060	SS
20	GRNN 4-51-4-3	0,7968	0,9726	0,8098	0,0054	0,0067	0,0058	SS
21	GRNN 6-51-4-3	0,5889	1,0025	0,6816	0,0041	0,0068	0,0048	SS
22	GRNN 10-51-4-3	0,3672	1,0292	0,7394	0,0029	0,0067	0,0052	SS
23	GRNN 12-51-4-3	0,0954	1,0972	0,7312	0,0011	0,0069	0,0051	SS

Linear – linear neural network
MLP – multilayer perceptron
RBF – radial basis function neural network
GRNN – general regression neural network
PI – pseudoinversion (neural network training algorithm)
BP - backpropagation error (neural network training algorithm)
CG - conjugate gradient (neural network training algorithm)
KM - *k*-means (neural network training algorithm)
KN - *k*-neighbors (neural network training algorithm)
SS – subsample (neural network training algorithm)

Linear networks tested demonstrated relatively simple net topologies – input and outputs, without hidden layer. Their modeling abilities, described by quality for validating subset, are rather poor and stable (0,9436–0,9876), even in case of systematically lowering the net input number from 12 to 4 only. Significant improvement of the model quality is observed in case of multilayer perceptrons (MLPs), where change of the neuron's transfer function (from linear into sigmoid) and introduction of hidden layer with hidden neurons developed and improved the net modeling properties clearly. Quality indicator for validating subset improved visibly (0,7869–0,9171). However, addition of second hidden layer, with different combinations of total number of hidden neurons and their distribution within both hidden layers, was not correlated with clear improvement of the net performance (quality indicator varied within the 0,8362–0,9388 range). Radial basis function networks (RBFs), considering quality indicator (0,9680–1,1831) seemed to be not adequate for this problem modeling. Similarly, the general regression neural networks (GRNNs) demonstrated approaching level of quality indicator (0,9588–1,0972). Moreover, considering number of hidden neurons (55) in all configurations tested, their generalization and regression abilities (interpolation, extrapolation) can be problematic.

Optimal neural network structure was identified based on minimal value of quality indicator for validating subset (see No 8 in Table 2). Moreover, also some proportion/deviation between quality indicators for training, validating and testing subsets was additionally analyzed (demanded proportional trends in all three quality indicators values, possibly similar values, avoiding contradictory trends). The optimal net structure was multilayer perceptron (MLP) with 12 inputs, one hidden layer with 11 neurons and 3 outputs representing three temperatures: IDT, HT and FT. This optimal configuration was trained in supervised mode using hybrid training scheme – initially with 100 iterations with fundamental backpropagation (BP) error algorithm, followed by the next 34 iterations with other algorithm (conjugate gradient, CG). Statistical characteristic of the neural model in respect to three outputs – predicted ash melting temperatures IDT, HT and FT – is presented in Table 3. This neural network configuration is presented in Fig. 1 (as 3-output neural IDT-HT-FT model).

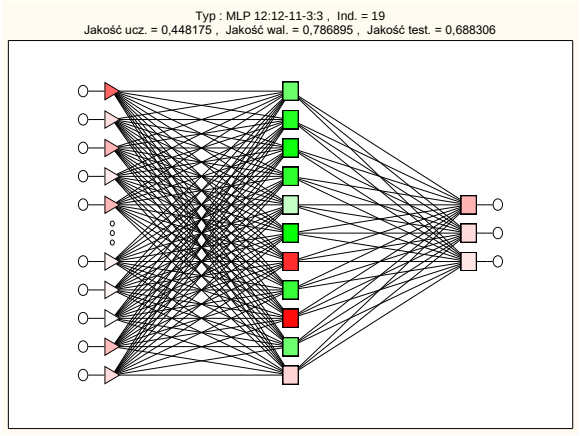

Fig. 1 Scheme of the artificial neural network used as the numerical IDT-HT-FT model.

Construction and practical verification of other, more specialized models, with one output only (representing IDT or HT or FT), denoted as IDT model, HT model and FT model, respectively (additional 300 dedicated working configurations tested – 100 ones for IDT model, 100 ones for HT model and 100 ones for FT model), resulted in similar statistical characteristics (Table 3). The general IDT-HT-FT model (3 outputs) and specialized 1-output models (IDT model, HT model, FT model) demonstrated the following R^2: IDT 0,615 and 0,064 – 0,637, HT 0,756 and 0,179 – 0,810, as well as FT 0,729 and 0,004 – 0,724, appropriately. One can thus conclude, that quality of 3-output model and of three individually specialized 1-output models is roughly identical and specific structure and dispersion of the data in hyperspace cannot be in computational practice transformed better using the best-specialized, dedicated 1-output models. On the other hand, considering the reported [19] difficulties in identification of any correlation within the data and the correlations with $R^2 < 0,708$

achievable with the use of classical regression methods, the R^2 presented in Table 3 can be regarded comparable or even better.

Table 3
Statistical characteristics of neural networks representing the IDT-HT-FT, as well as the IDT, HT and FT models in respect to model outputs: IDT, HT and FT

	Model No 8 (see Table 2) representing the best configuration from within 100 of 3-outputs configurations tested			Min and max values from within 100 working network configurations tested	Min and max values from within 100 working network configurations tested	Min and max values from within 100 working network configurations tested
	IDT-HT-FT model parameters in respect to:			IDT model	HT model	FT model
	IDT [°C]	HT [°C]	FT [°C]	IDT [°C]	HT [°C]	FT [°C]
Mean error	6,349	3,096	-10,035	-29,744 – 31,342	-19,553 – 26,017	-25,895 – 34,82
Error deviation	109,997	65,178	61,051	107,595 – 188,493	60.961 – 168,029	62,392 – 157,194
Mean absolute error	76,018	51,557	46,342	62,215 – 150,625	38,106 – 127,194	46,388 – 102,821
Correlation	0,785	0,869	0,854	0,252 – 0,798	0,423 – 0,900	0,063 – 0,851
R^2	0,615	0,756	0,729	0,064 – 0,637	0,179 – 0,810	0,004 – 0,724

In general 400 neural network configurations were considered, including 100 net topologies representing IDT-HT-FT model, 100 for IDT model, 100 for HT model and 100 for FT model, respectively.

Comparing the data in Table 1 and 3 concerning the three predicted parameters – ash melting temperatures – one can conclude, that because of intrinsic dispersion of the original data (standard deviation in respect to each temperature parameter – see Table 1: IDT 177,806°C, HT 132,221°C and FT 117,568°C) the comparable parameter (error deviation) values – see Table 3: IDT 109,997°C, HT 65,178°C and FT 61,051°C are even smaller. This observation suggests, that further lowering of the model prediction error is not theoretically motivated and that model quality has already reached its allowable limits resulting from raw data structure and dispersion. Further lowering of error deviations values (model performance) compared to standard deviations (raw training/validation/testing data structure) may also be responsible for unwanted model effects since the neural network model will render, besides identification of main trends within the data, also some other less important correlations and connections within the data (information noise, sampling errors, etc.). This way further improvement of the net model quality is - under these conditions - not recommended.

Graphical comparison of the experimental data and neural network IDT-HT-FT model predictions is presented in Fig. 2a-c.

a)

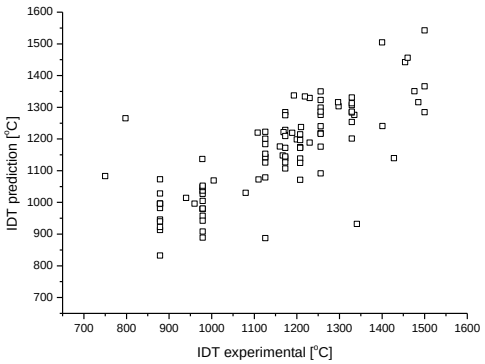

b)

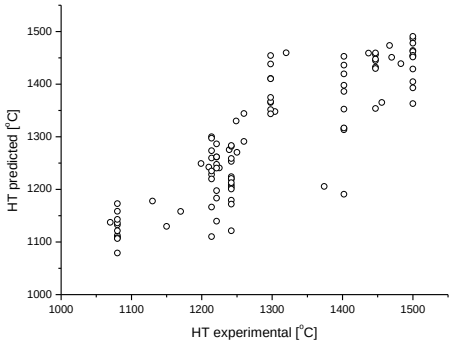

c)

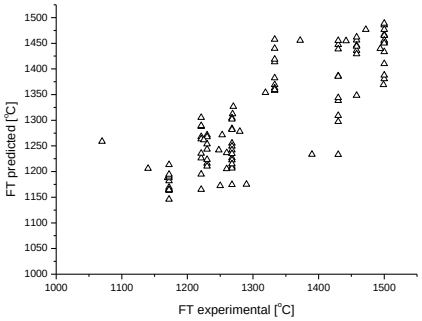

Fig. 2 Comparison of experimental data and values predicted by neural network IDT-HT-FT model (a – IDT temperature, b) HT temperature, c) FT temperature).

Sensitivity of the 3-output IDT-HT-FT neural network model in respect to individual inputs is presented in Table 4. Sensitivity tests were based on identification of model prediction error after systematic, individual removal of each parameter one time from within the original 12 input parameters set.

Table 4
Sensitivity analysis of the neural network 3-output IDT-HT-FT model in respect to individual inputs.

Input	Rank	Error increment
K_2O	1	1,3521
SiO_2	2	1,3478
CaO	3	1,1292
Al_2O_3	4	1,1000
SO_3	5	1,0581
S_d (in biomass)	6	1,0358
P_2O_5	7	1,0335
Fe_2O_3	8	1,0320
Na_2O	9	1,0255
TiO_2	10	1,0221
MgO	11	1,0177
Cl (in biomass)	12	0,9969

From the data presented in Table 4 one can see, that the most important parameter affecting the three temperatures is K_2O and SiO_2 content, with error increments as 1,3521 and 1,3478, appropriately (rank 1 and 2). Both K_2O and SiO_2 contents are practically equally important for ash melting temperatures. Second group, of moderate importance in respect to three net outputs, is represented by CaO and Al_2O_3 contents (rank 3, error increment 1,1292 and rank 4 with error increment 1,1000). The last, however broad group of the lowest impact on the model predictions, is represented by: SO_3, S_d (in biomass), P_2O_5, Fe_2O_3, Na_2O, TiO_2 and MgO (ranks 5 – 11, error increment

range of 1,0581–1,0177). The last parameter (rank 12) can be regarded to be neutral in respect to model performance, suggesting minimal impact of Cl (in biomass) on the three ash melting temperatures. Moreover, in last case removal of this parameter (Cl) from the model inputs results in practically unmodified performance, and even improvement of statistical characteristic of the model (error increment < 1).

It is also interesting to make sensitivity analysis in respect to individual ash melting temperatures, what can be done analyzing the performance of three 1-output models. The resulting data are presented in Table 5.

Table 5

Sensitivity analysis of the 1-output neural network models (representing individual ash melting temperatures: IDT, HT and FT) in respect to individual inputs.

IDT model[1]			HT model[2]			FT model[3]		
Input	Rank	Error increment	Input	Rank	Error increment	Input	Rank	Error increment
SiO_2	1	1,2495	K_2O	1	1,5674	CaO	1	1,3834
Al_2O_3	2	1,1982	SiO_2	2	1,4255	SiO_2	2	1,3091
CaO	3	1,1905	CaO	3	1,4172	K_2O	3	1,2240
K_2O	4	1,0751	Al_2O_3	4	1,2526	Al_2O_3	4	1,1979
SO_3	5	1,0726	Na_2O	5	1,1442	TiO_2	5	1,1921
S_d	6	1,0569	P_2O_5	6	1,0971	Na_2O	6	1,1571
P_2O_5	7	1,0469	S_d	7	1,0550	MgO	7	1,1451
TiO_2	8	1,0441	Cl	8	1,0336	P_2O_5	8	1,1114
Cl	9	1,0039	MgO	9	1,0267	Fe_2O_3	9	1,0453
MgO	10	1,0019	SO_3	10	1,0123	S_d	10	1,0332
Fe_2O_3	11	0,9995	Fe_2O_3	11	1,0098	Cl	11	1,0091
Na_2O	12	0,9399	TiO_2	12	0,9684	SO_3	12	0,9893

[1] IDT model: MLP 12-9-1, training set quality: 0,2488, validating set quality 0,5566, testing set quality 1,2559, training set error 0,0605, validating set error 0,1164, testing set error 0,2877, training algorithms sequence: BP 100 iterations + CG 65 iterations

[2] HT model: MLP 12-7-1, training set quality 0,3475, validating set quality 0,6297, testing set quality 0,8207, training set error 0,0914, validating set error 0,1441, testing set error 0,1876, training algorithms sequence: BP 100 iterations + CG 26 iterations

[3] FT model: MLP 12-12-1, training set quality 0,2827, validating set quality 0,4494, testing set quality 0,7727, training set error 0,0630, validating set error 0,1096, testing set error 0,1607, training algorithms sequence: BP 100 iterations + CG 49 iterations

Comparing and analyzing the data in Table 5 one can identify sensitivity towards input parameters (ash chemical components) in respect to each ash melting temperature individually. It is visible, that each characteristic temperature – IDT, HT and FT – demonstrates slightly different hierarchy of model inputs significance.

Exemplary presentation of the model performance – simulation of simultaneous effect of SiO_2 (15–45%, dry weight basis) and Al_2O_3 (4–12%) changes (proportions) assuming constant values of: CaO (15%), K_2O (15%), MgO (4%), Fe_2O_3 (1,5%), SO_3 (3%), Na_2O (1%), TiO_2 (0,2%), S_d (in biomass) (0,05%) and Cl (in biomass) (0,05%) fractions, with P_2O_5 fraction representing the rest to 100% is presented in Fig. 3a-c. It should be emphasized, that the observed smooth response surface speaks also for properly trained model network structure, without dominating overtraining effects demonstrating themselves as the surface oscillations, etc.

It should be noted, that different combinations of constant (parameters) values can modify the SiO_2- Al_2O_3 projection (even considerably) since all 12 inputs affect simultaneously and collectively (with higher or lower impact resulting from strength of interneuron connections – see Tables 4-5, activation levels of transfer function depending on bias values, etc.) the modeled output parameters representing three characteristic ash melting temperatures.

a)

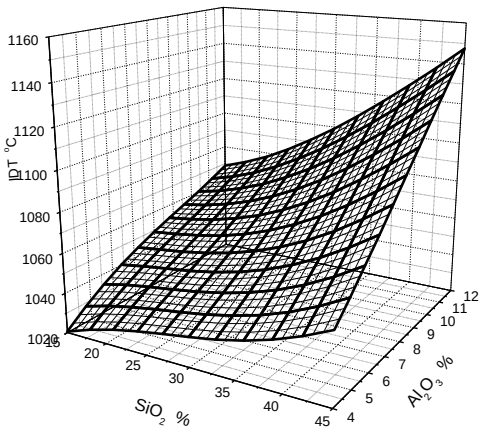

b)

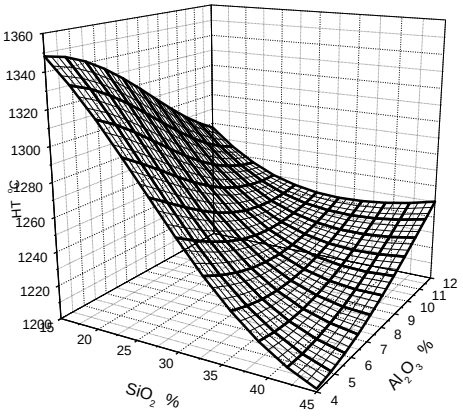

c)

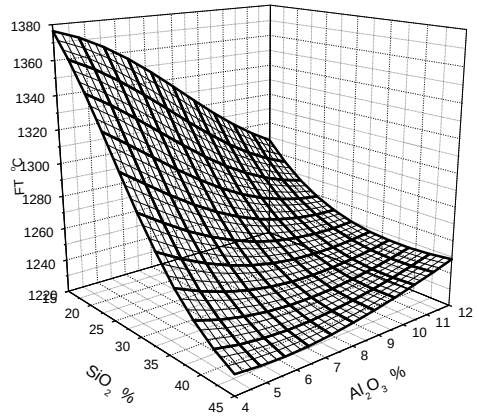

Fig. 3 Simultaneous effect of SiO_2 (15–45%) and Al_2O_3 (4–12%) proportions - assuming constant values of: CaO (15%), K_2O (15%), MgO (4%), Fe_2O_3 (1,5%), SO_3 (3%), Na_2O (1%), TiO_2 (0,2%), S_d (in biomass) (0,05%) and Cl (in biomass) (0,05%) fractions and P_2O_5 fraction

representing the rest to 100% - on IDT (a), HT (b) and FT (c) ash fusion temperatures – graphical presentation of neural network IDT-HT-FT model predictions.

Conclusions

Artificial neural network model was proposed for prediction of ash melting temperatures based on chemical composition of the ash derived from biomass burning. Such ash properties are key indicators in selection of alternative processing routes according to Circular Economy technologies.

Statistical indicators suggest, that considering the intrinsic dispersion within the original data structure, the results provided by the model can be regarded acceptable. However, considering reported in literature quality of various statistical approaches using classical regression methods and combinations of some indicators, quality of the demonstrated neural network model can be regarded as comparable or even better.

To improve interpolation and extrapolation abilities of the model, more parameters potentially affecting the process should be considered and model construction development on this basis should be continued. Especially some parameters characterizing e.g. char structure may be considered, providing thus better modeling insight into simultaneous mass (diffusion/convection) and heat transfer in this heterogeneous reacting system, affecting indirectly environment of the chemical reactions selectivity, kinetics and phase changes.

However, neural network model in its present form can be also used as efficient tool in some computational works or predictive simulations in energetic applications of biomass required by Industry 4.0 strategy.

Acknowledgement

The research presented in this paper was performed within “Process optimisation and valorisation of combustion by-products in transition to circular economy’ (UPS-Plus) funded by The Foundation for Polish Science (FNP) within Team Teach Core Facility Programme, No PO IR 4.4 (2018–2021).

References

[1] J.L. Míguez, J.C. Morán, E. Granada, J. Porteiro, Review of technology in small-scale biomass combustion systems in the European market, Renewable and Sustainable Energy Reviews 16 (2012) 3867–3875.

[2] M. Sajdak, M. Kmieć, B. Micek, J. Hrabak, Determination of the optimal ratio of coal to biomass in the co-firing process: feed mixture properties, International Journal of Environmental Science and Technology 16 (2019) 2989–3000.

[3] L.J.R. Nunes, J.C.O. Matias, J.P.S. Catalão, Biomass combustion systems: A review on the physical and chemical properties of the ashes, Renewable and Sustainable Energy Reviews 53 (2016) 235–242.

[4] S.V. Vassilev, D. Baxter, L.K. Andersen, C.G. Vassileva, An overview of the composition and application of biomass ash. Part 1. Phase-mineral and chemical composition and classification, Fuel 105 (2013) 40–76.

[5] S. Du, H. Yang, K. Qian, X. Wang, H. Chen, Fusion and transformation properties of the inorganic components in biomass ash, Fuel 117 (2014) 1281–1287.

[6] S.V. Vassilev, D. Baxter, C.G. Vassileva, An overview of the behavior of biomass during combustion: Part II. Ash fusion and ash formation mechanisms of biomass types, Fuel 117 (2014) 152–183.

[7] S.V. Vassilev, C.G. Vassileva, Y.-C. Song, W.-Y. Li, J. Feng, Ash contents and ash-forming elements of biomass and their significance for solid biofuel combustion, Fuel 208 (2017) 377–409.

[8] M. Roman, E. Bobaşu, D. Selişteanu, Modelling of biomass combustion process, Energy Procedia 6 (2011) 432–440.

[9] L. Wang, Ø. Skreiberg, M. Becidan, H. Li, Investigation of rye straw ash sintering characteristics and the effect of additives, Applied Energy 162 (2016) 1195–1204.

[10] L. Ding, Y. Gong, Y. Wang, F. Wang, G. Yu, Characterisation of the morphological changes and interactions in char, slag and ash during CO_2 gasification of rice straw and lignite, Applied Energy 195 (2017) 713–724.

[11] L. Wang, J.E. Hustad, Ø. Skreiberg, G. Skjevrak, M. Grønli, A critical review on additives to reduce ash related operation problems in biomass combustion applications, Energy Procedia 20 (2012) 20–29.

[12] Y. Qin, M. Feng, Z. Zhao, S.V. Vassilev, J. Feng, C.G. Vassileva, W. Li, Effect of biomass ash addition on coal ash fusion process under CO_2 atmosphere, Fuel 231 (2018) 417–426.

[13] R.K. Sandhu, R. Siddique, Influence of rice husk ash (RHA) on the properties of self-compacting concrete: A review, Construction and Building Materials 153 (2017) 751–764.

[14] H. Zhou, W. Ma, An experimental study on the effects of adding biomass ashes on ash sintering behavior of Zhundong coal, Applied Thermal Engineering 126 (2017) 689–701.

[15] S. Voshell, M. Mäkelä, O. Dahl, A review of biomass ash properties towards treatment and recycling, Renewable and Sustainable Energy Reviews 96 (2018) 479–486.

[16] L. Reijnders, Disposal, uses and treatments of combustion ashes: a review, Resources, Conservation and Recycling 43 (2005) 313–336.

[17] S.V. Vassilev, D. Baxter, L.K. Andersen, C.G. Vassileva, An overview of the composition and application of biomass ash. Part 2. Potential utilisation, technological and ecological advantages and challenges, Fuel 105 (2013) 19–39.

[18] R. Xiao, X. Chen, F. Wang, G. Yu, The physicochemical properties of different biomass ashes at different ashing temperature, Renewable Energy 36 (2011) 244–249.

[19] A. Garcia-Maraver, J. Mata-Sanchez, M. Carpio, J.A. Perez-Jimenez, Critical review of predictive coefficients for biomass ash deposition tendency, Journal of the Energy Institute, 90 (2017) 214–228.

[20] T. Rizvi, P. Xing, M. Pourkashanian, L.I. Darvell, J.M. Jones, W. Nimmo, Prediction of biomass ash fusion behaviour by the use of detailed characterization methods coupled with thermodynamic analysis, Fuel 141 (2015) 275–284.

[21] K. Piotrowski, J. Piotrowski, J. Schlesinger, Modelling of complex liquid-vapour equilibria in the urea synthesis process with the use of artificial neural network, Chemical Engineering and Processing, 42(4) (2003) 285–289.

[22] T. Wiltowski, K. Piotrowski, H. Lorethova, L. Stonawski, K. Mondal, S.B. Lalvani, Neural network approximation of iron oxide reduction process, Chemical Engineering and Processing, 44(7) (2005) 775–783.

[23] K. Piotrowski, T. Wiltowski, K. Mondal, L. Stonawski, T. Szymanski, D. Dasgupta, Simultaneous influence of gas mixture composition and process temperature on $Fe_2O_3 \rightarrow FeO$ reduction kinetics – neural network modeling, Brazilian Journal of Chemical Engineering, 22(3) (2005) 419–432.

[24] J. Piotrowski, K. Piotrowski, B. Lipowska, Neural network modelling of $NaNO_2$ inversion process kinetics, Polish Journal of Chemical Technology, 6(1) (2004) 37–41.

[25] K. Piotrowski, B. Wierzbowska, J. Koralewska, A. Matynia, Influence of methanol and ethanol on vitamin C crystallization temperature – neural network model, Pol. J Chem. Technol., 8(4) (2006) 23–26.

[26] K. Piotrowski, J. Koralewska, B. Wierzbowska, A. Matynia, Kinetics of the continuous reaction crystallization of barium sulphate in $BaCl_2 – (NH_4)_2SO_4 – NaCl – H_2O$ system – neural network model, Polish Journal of Chemical Technology, 11(4) (2009) 13–19.

[27] K. Piotrowski, N. Hutnik, A. Matynia, Effect of sulphate(VI) ions on CSD of struvite – neural network model of continuous reaction crystallization process in a DT MSMPR crystallizer, Procedia Engineering, 42 (2012) 573–584.

[28] K. Piotrowski, A. Matynia, N. Hutnik, Gas-liquid jet pump crystallizer in phosphorus recycling technology – neural network model, Procedia Environmental Sciences, 18 (2013) 756–765.

[29] O.B. Douma, B. Boukhatem, M. Ghrici, A. Tagnit-Hamou, Prediction of properties of self-compacting concrete containing fly ash using artificial neural network, Neural Comput. & Applic. 28 (Suppl 1) (2017) S707–S718.

[30] A. Najigivi, A. Khaloo, A. Iraji zad, S.A. Rashid, An artificial neural networks model for predicting permeability properties of nano silica – rice husk ash ternary blended concrete, International Journal of Concrete Structures and Materials 7(3) (2013) 225–238.

[31] S. Subaşi, Prediction of mechanical properties of cement containing class C fly ash by using artificial neural network and regression technique, Scientific Research and Essay 4(4) (2009) 289–297.

[32] O. Karahan, H. Tanyildizi, C.D. Atis, An artificial neural network approach for prediction of long-term strength properties of steel fiber reinforced concrete containing fly ash, Journal of Zhejiang University SCIENCE A, 9(11) (2008) 1514–1523.

[33] Y. Kellouche, B. Boukhatem, M. Ghrici, A. Tagnit-Hamou, Exploring the major factors affecting fly-ash concrete carbonation using artificial neural network, Neural Computations & Application, 31(Suppl 2) (2019) S969–S988.

[34] J. Bai, S. Wild, J.A. Ware, B.B. Sabir, Using neural networks to predict workability of concrete incorporating metakaolin and fly ash, Advances in Engineering Software, 34 (2003) 663–669.

[35] M. Gulec, E. Gulbandilar, Determination of the lower calorific and ash values of the lignite coal by using artificial neural networks and multiple regression analysis, Physicochemical Problems of Mineral Processing, doi: 10.5277/ppmp18149 (2018) 1–7.

[36] G. Li, Z. Liu, J. Li, Y. Fang, J. Shan, S. Guo, Z. Wang, Modeling of ash agglomerating fluidized bed gasifier using back propagation neural network based on particle swarm optimization, Applied Thermal Engineering, 129 (2018) 1518–1526.

[37] I. Siregar, Y. Niu, P. Mostaghimi, R.T. Armstrong, Coal ash content estimation using fuzzy curves and ensemble neural networks for well log analysis, International Journal of Coal Geology, 181 (2017) 11–22.

[38] S.D. Saravanan, M. Senthilkumar, Prediction of tribological behaviour of rice husk ash reinforced aluminum alloy matrix composites using artificial neural network, Russian Journal of Non-Ferrous Metals, 56(1) (2015) 97–106.

[39] A. Nazari, Artificial neural networks for prediction compressive strength of geopolymers with seeded waste ashes, Neural Computing & Applications, 23 (2013) 391–402.

[40] S. Miao, Q. Jiang, H. Zhou, J. Shi, Z. Cao, Modeling and prediction of coal ash fusion temperature based on BP neural network, MATEC Web of Conferences 40 (2016) 05010, DOI: 10.1051/matecconf/20164005010.

[41] Y.P. Liu, M.G. Wu, J.X. Qian, Predicting coal ash fusion temperature based on its chemical composition using ACO-BP neural network, Thermochimica Acta 454 (2007) 64–68.

[42] C. Yin, Z. Luo, M. Ni, K. Cen, Predicting coal ash fusion temperature with a back-propagation neural network model, Fuel 77(15) (1998) 1777–1782.

[43] Report from BioEffGen Project “Advanced pretreat-ment and characterization of Biomass for Efficient Generation of heat and power” (BioEf-fGen) funded by The National Centre for Research and Development within Polish-German Sustainability Research Programme (STAIR)

[44] P. Sakiewicz, J. Cebula, K. Piotrowski, R. Nowosielski, R. Wilk, M. Nowicki, Application of micro- and nanostructural multifunctional halloysite-based sorbents from DUNINO deposit in selected biotechnological processes, Journal of Achievements in Materials and Manufacturing Engineering, 69(2) (2015) 69–78.

[45] P. Sakiewicz, R. Nowosielski, W. Pilarczyk, K. Gołombek, M. Lutyński, Selected properties of the halloysite as a component of Geosynthetic Clay Liners (GCL), Journal of Achievements in Materials and Manufacturing Engineering, 48(2) (2011) 177–191.

[46] P. Sakiewicz, M. Lutyński, J. Sołtys, A. Pytliński, Purification of halloysite by magnetic separation, Physicochemical Problems of Mineral Processing 52(2) (2016) 991–1001.